Robotica (2017) volume 35, pp. 2381–2399. © Cambridge University Press 2017
doi:10.1017/S026357471700008X

In-hand forward and inverse kinematics with rolling contact

Lei Cui†*, Jie Sun‡ and Jian S. Dai‡

† *Department of Mechanical Engineering, Curtin University, Perth, Australia*
‡ *Centre for Robotics Research, King's College London, London, UK.*
E-mails: jie.sun@kcl.ac.uk, jian.dai@kcl.ac.uk

(Accepted February 04, 2017. First published online: February 27, 2017)

SUMMARY
Robotic hands use rolling contact to manipulate a grasped object to a desired location, even when the finger and the palm linkage mechanisms lack degrees of freedom. This paper presents a systematic approach to the forward and inverse kinematics of in-hand manipulation. The moving frame method in differential geometry is integrated into the product of exponential formula to establish a pure geometric framework of the kinematics of a robot hand. The forward and inverse kinematics of a multifingered hand are obtained in terms of the joint rates and contact trajectories. A two-fingered planar robot hand and a three-fingered spatial robot hand are used to demonstrate the proposed approach. The proposed formulation amounts to solving a univariate polynomial, providing an alternative to the existing ones that require numerical integration.

KEYWORDS: Contact; Rolling, Kinematics; Multifingered hands; Manipulation; Product of exponential; Moving frame method.

1. Introduction

In-hand manipulation involves manipulating a grasped object by a robot hand by itself. Rolling contact between the fingertips and the object can be exploited to enlarge the reachable workspace and simplify control. Rolling contact imposes nonholonomic constraints, where the equations relating two smooth bodies are expressed in terms of their velocities. The kinematics of rolling contact is essential for the subsequent development of path planning and control.

An increasing number of robotic hands use tactile fingertips, which shifts the focus of robot hand studies from grasping to in-hand manipulation.[1] Re-grasp or finger gaiting, which entails the change of the grasping configuration of the robot hands, is one of the techniques for in-hand manipulation. Re-grasp consists of a sequence of pick-and-place operations, for example repositioning some fingers while maintaining grasping,[2] utilizing external factors such as gravity,[3] or throwing and re-catching the object,[4] for the object to reach the desired configuration.[5–9]

A more natural strategy for in-hand manipulation involves rotation, which typifies the dexterity of the human hand.[10,11] Robot hands are developed to emulate the movements of the human hand, so rolling contact for in-hand manipulation has received extensive studies.[12–17] Kinematics of rolling contact is a problem of nonholonomic constraint in terms of velocities, and thus, the formulations of in-hand manipulation consider the shapes of the grasped object and the fingertips.[18–26]

In literature, kinematics of rolling contact can be divided into two broad categories: pure-rolling motion and spin-rolling motion. The object under pure-rolling contact has two degrees of freedom (DOFs) with its two instantaneous rotation axes parallel to the common tangent plane of two objects. The object under spin-rolling contact has three DOFs with its instantaneous rotation axes in any arbitrary directions. The spin-rolling contact is also called twist-rolling contact and/or simply rolling contact.[19,24,27]

* Corresponding author. E-mail: lei.cui@curtin.edu.au

Slide-twist-rolling may occur in in-hand manipulation. Theoretical works on modelling dexterous manipulation with sliding fingers have been presented in ref. [28, 29]. However, tactile sensors that can keep track the onset slip are still in the early stage of development.[30,31] The current strategy is to prevent sliding from happening.[32]

A useful kinematic formulation of multifingered hands should consider computational efficiency and the ease with which it can be manipulated. Further, it should be flexible enough to admit a degree of coordinate independence, i.e. a given problem should not be confined to any specific choice of reference frames to carry out the kinematic analysis.

Motivated in part by these considerations, the product of exponential formula[33−35] has been widely used in analysing kinematics of multifingered hands.[33,36−39] However, since kinematics of rolling contact is traditionally derived in terms of the coordinates of surface patches, these coordinates inevitably appear in the in the kinematic formulations. This to some extent compromises the initial motivation.[40]

The moving frame method in differential geometry is a powerful geometric tool for exploring the geometric properties and invariants of submanifolds.[41,42] The Frenet–Serret frame provides a complete kinematic description of curves and leads to a complete classification of smooth curves in Euclidean space.[43] The Darboux frame extends the Frenet–Serret frame from a curve to a surface in Euclidean space.[44] The moving frame method was later developed extensively by Cartan and others in the study of submanifolds of more general homogeneous spaces.[41]

This work presents a systematic approach to the kinematics of in-hand manipulation with rolling contact, where the Darboux frame, which moves along a locus on each of a fingertip surface and an object surface,[19,21,22] is applied to the forward and inverse kinematics of the moving object. The integration of the product of exponential and the moving frame method yields an algebraic formulation, providing an alternative to a differential equation approach.

The rest of the paper is organized as follows. Sections 2 and 3 derive the forward and inverse kinematics of a multifingered robot hand, respectively. Section 4 shows the application of the proposed approach to a two-fingered planar hand with planar end-effectors manipulating a disc. Section 5 shows a three-fingered hand with ellipsoidal fingertips manipulating an ellipsoidal object. Section 6 discussed the application of the proposed approach with the three-fingered MetaHand. Section 7 concludes this work.

2. Forward Kinematics of In-Hand Manipulation with Rolling Contact

We made three assumptions when obtaining the twist of the object under the effects of joint motion of fingers and rolling contact. The first assumption is the system consists of a multifingered hand and an object, where the fingertips and the object maintain rolling contact. The second assumption is the contact trajectories of the fingers are within the workspace of the robot hand. The third assumption is the fingertip and the object surfaces have partial derivatives up to the second order, and continuous Gauss curvatures exist.

When the fingertip surface maintains rolling contact with the object surface, the point of contact moves across both surfaces, and the object undergoes a three-DOF spin-rolling motion with respect to the fingertips. Each fingertip has to follow the object and maintain contact. The grasp constraints analysis during manipulating an object has been presented before,[45,46] hence the motion of a single finger is examined in this work.

Let (P-$\boldsymbol{ijk}$) represent a frame fixed at the palm, (T-$\boldsymbol{i'j'k'}$) a tool frame fixed on the fingertip, and (O-$\boldsymbol{i''j''k''}$) an object frame, $\boldsymbol{S}_1$ to $\boldsymbol{S}_n$ the screws related to the revolute joints, M the contact point, L and L' the contact trajectories, respectively, on the fingertip and on the object, $\boldsymbol{e}_1$ the common tangent vector of L and L', and $\boldsymbol{e}_3$ the common normal vector of the two surfaces, as in Fig. 1.

The tool frame (T-$\boldsymbol{i'j'k'}$) on the fingertip with respect to the palm frame (P-$\boldsymbol{ijk}$) can be obtained by the product of exponential formula[33] in terms of joint angles η_1 to η_n as

$$\boldsymbol{g}_{PT} = e^{\boldsymbol{S'}_1\eta_1} e^{\boldsymbol{S'}_2\eta_2} \ldots e^{\boldsymbol{S'}_n\eta_n} \boldsymbol{g}_{PT}(0) \tag{1}$$

where $\boldsymbol{S'}_i = \mathrm{Ad}_{e^{\mathrm{S}_1\eta_1} e^{\mathrm{S}_2\eta_2} \ldots e^{\mathrm{S}_{i-1}\eta_{i-1}}} \boldsymbol{S}_i$, and $\boldsymbol{S}_i$ is the screw of the ith joint in the initial configuration. The matrix $\boldsymbol{g}_{PT}(0)$ is the initial location of the frame (T-$i'j'k'$). The twist of the frame (T-$i'j'k'$) with

https://doi.org/10.1017/S026357471700008X Published online by Cambridge University Press

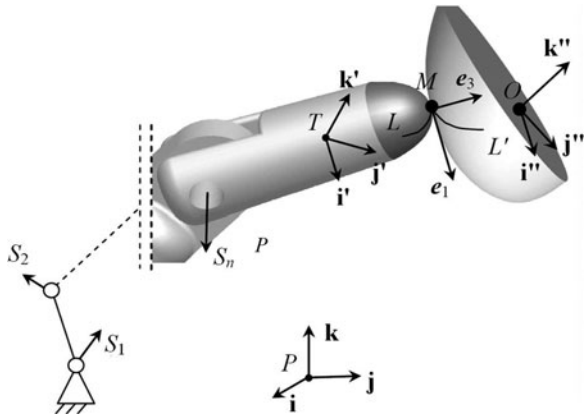

Fig. 1. The joint screws $\boldsymbol{S}_1$ to $\boldsymbol{S}_n$, tool frame (T-$i'j'k'$), and the Darboux frame (M-$\boldsymbol{e}_1\boldsymbol{e}_2\boldsymbol{e}_3$) of a single finger.

respect to the frame (P-ijk) can be obtained as

$$\boldsymbol{S}_{PT} = \dot{\boldsymbol{g}}_{PT}\boldsymbol{g}_{PT}^{-1} = \boldsymbol{J}(\boldsymbol{\eta})\dot{\boldsymbol{\eta}} \tag{2}$$

where $\boldsymbol{J}(\boldsymbol{\eta}) = [\,\boldsymbol{S}'_1\ \boldsymbol{S}'_2\ \ldots\ \boldsymbol{S}'_n\,]$ and $\dot{\boldsymbol{\eta}} = [\,\dot{\eta}_1\ \dot{\eta}_2\ \ldots\ \dot{\eta}_n\,]^T$

The homogeneous matrix of the frame (M-$\boldsymbol{e}_1\boldsymbol{e}_2\boldsymbol{e}_3$) with respect to the tool frame (T-$i'j'k'$) is

$$\boldsymbol{g}_{TM} = \begin{bmatrix} \mathbf{E} & \boldsymbol{M} \\ 0 & 1 \end{bmatrix} \tag{3}$$

where $\mathbf{E} = [\,\boldsymbol{e}_1^T\ \boldsymbol{e}_2^T\ \boldsymbol{e}_3^T\,]$ and the vector $\boldsymbol{M}$ is the position vector of the point M with respect to the frame (T-$i'j'k'$). Please note that we followed the convention that the vectors $\boldsymbol{e}_1$ to $\boldsymbol{e}_3$ of the Darboux frame are row vectors.[41,42]

The differentiation of the matrix **E**with respect to time t yields

$$\frac{\mathrm{d}\mathbf{E}}{\mathrm{d}t} = \frac{\mathrm{d}\mathbf{E}}{\mathrm{d}s}\frac{\mathrm{d}s}{\mathrm{d}t} = \sigma\boldsymbol{\Omega}\mathbf{E} \tag{4}$$

where s is the arc length and $\sigma = \mathrm{d}s/\mathrm{d}t$ is the rolling rate of the contact curve L, and

$$\boldsymbol{\Omega} = \begin{bmatrix} 0 & k_g & k_n \\ -k_g & 0 & \tau_g \\ -k_n & -\tau_g & 0 \end{bmatrix} \tag{5}$$

The scalars k_g, k_n, and τ_g are the geodesic curvature, normal curvature, and geodesic torsion of the contact curve L in the direction of $\boldsymbol{e}_1$, respectively. The differentiation $\boldsymbol{M}$ with respect to t yields

$$\frac{\mathrm{d}\boldsymbol{M}}{\mathrm{d}t} = \frac{\mathrm{d}\boldsymbol{M}}{\mathrm{d}s}\frac{\mathrm{d}s}{\mathrm{d}t} = \sigma\boldsymbol{e}_1^T \tag{6}$$

It follows that the differentiation of $\boldsymbol{g}_{TM}$ with respect to time t is

$$\dot{\boldsymbol{g}}_{TM} = \sigma\begin{bmatrix} \boldsymbol{\Omega}\mathbf{E} & \boldsymbol{e}_1^T \\ \mathbf{0} & 0 \end{bmatrix} \tag{7}$$

The twist of the frame (M-$\boldsymbol{e}_1\boldsymbol{e}_2\boldsymbol{e}_3$) with respect to the frame (T-$i'j'k'$) can be obtained as

$$\boldsymbol{V}_{TM} = \dot{\boldsymbol{g}}_{TM}\boldsymbol{g}_{TM}^{-1} = \sigma\begin{bmatrix} \boldsymbol{\Omega}\mathbf{E} & \boldsymbol{e}_1^T \\ \mathbf{0} & 0 \end{bmatrix}\begin{bmatrix} \mathbf{E}^T & -\mathbf{E}^T\boldsymbol{M} \\ \mathbf{0} & 1 \end{bmatrix} = \sigma\begin{bmatrix} \boldsymbol{\Omega} & \boldsymbol{e}_1^T - \boldsymbol{\Omega}\mathbf{M} \\ \mathbf{0} & 0 \end{bmatrix} \tag{8}$$

https://doi.org/10.1017/S026357471700008X Published online by Cambridge University Press

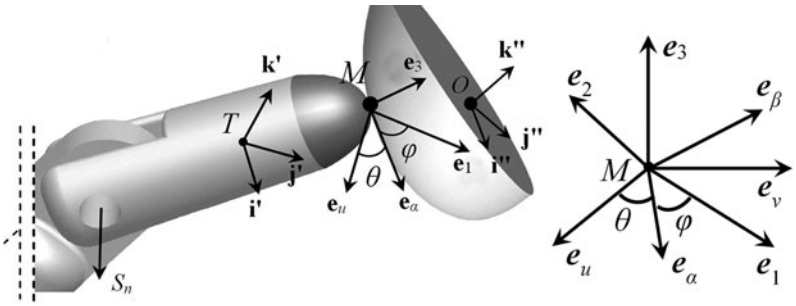

Fig. 2. The Douboux frames (M-$\boldsymbol{e}_u\boldsymbol{e}_v\boldsymbol{e}_3$), ($M$-$\boldsymbol{e}_\alpha\boldsymbol{e}_\beta\boldsymbol{e}_3$), and ($M$-$\boldsymbol{e}_1\boldsymbol{e}_2\boldsymbol{e}_3$).

It follows that the twist of the frame M with respect to the frame T is

$$\boldsymbol{S}_{TM} = \begin{bmatrix} \sigma \boldsymbol{e}_1^T + \boldsymbol{M} \times \boldsymbol{\omega}_M \\ \boldsymbol{\omega}_M \end{bmatrix} \tag{9}$$

where

$$\boldsymbol{\omega}_M = \sigma \left(-\tau_g \boldsymbol{e}_1 + k_n \boldsymbol{e}_2 - k_g \boldsymbol{e}_3 \right) \tag{10}$$

Remark: The first three elements of $\boldsymbol{S}_{TM}$ in Eq. (9) represent the linear velocity of the point M with respect to the frame (T-$i'j'k'$). This velocity is the combined effects of a velocity $\sigma \boldsymbol{e}_1^T$ induced by rolling and a velocity induced by rotation of the frame (M-$\boldsymbol{e}_1\boldsymbol{e}_2\boldsymbol{e}_3$).

The angular velocity of the object frame (O-$i''j''k''$) with respect to the frame (M-$\boldsymbol{e}_1\boldsymbol{e}_2\boldsymbol{e}_3$) [19] is

$$\boldsymbol{\omega}_O = \omega_1 \boldsymbol{e}_1 + \omega_2 \boldsymbol{e}_2 + \omega_3 \boldsymbol{e}_3 \tag{11}$$

where $\omega_1 = -\sigma(\tau'_g - \tau_g)$, $\omega_2 = \sigma(k'_n - k_n)$, $\omega_3 = -\sigma(k'_g - k_g)$, and τ'_g, k'_n, k'_g are the geodesic torsion, normal curvature, and geodesic curvature of the contact curve L' on the object, respectively. It follows that the twist of the object frame (O-$i''j''k''$) with respect to the frame (M-$\boldsymbol{e}_1\boldsymbol{e}_2\boldsymbol{e}_3$) is

$$\boldsymbol{S}_{MO} = \begin{bmatrix} \boldsymbol{O} \times \boldsymbol{\omega}_O \\ \boldsymbol{\omega}_O \end{bmatrix} \tag{12}$$

where the vector $\boldsymbol{O}$ represents the vector MO with respect to the frame (M-$\boldsymbol{e}_1\boldsymbol{e}_2\boldsymbol{e}_3$).

It follows from Eqs. (2), (9), and (12) that the twist of the object frame (O-$i''j''k''$) with respect to the palm frame (P-ijk) can be obtained as

$$\boldsymbol{S}_{PO} = \boldsymbol{S}_{PT} + \mathrm{Ad}_{\mathbf{g}_{PT}} \boldsymbol{S}_{TM} + \mathrm{Ad}_{\mathbf{g}_{PM}} \boldsymbol{S}_{MO} \tag{13}$$

This completes the forward kinematics of the robot hand under the effects of rolling contact and the joint rates.

3. Inverse Kinematics of In-Hand Manipulation with Rolling Contact

In this section, we obtain the inverse kinematics of multifingered hands under the effects of joint motion of fingers and rolling contact. Suppose that the surface of the fingertip is parameterized by $\boldsymbol{r}(u, v)$ and that of the object $\boldsymbol{r}'(\alpha, \beta)$. Let $\boldsymbol{e}_u$ represent the unit vector tangent to u-curve of the fingertip surface, $\boldsymbol{e}_\alpha$ the unit vector tangent to α-curve of the object surface, θ the angle between $\boldsymbol{e}_u$ and $\boldsymbol{e}_\alpha$ as in Fig. 2.

A general rigid object has six DOFs. Hence, the number of joints is at least three for a robotic finger to manipulate the object in a three-dimensional space, since rolling contact provides the other three terms to the system. In the authors' previous work, ref. [7], these three terms were defined

https://doi.org/10.1017/S026357471700008X Published online by Cambridge University Press

as the rolling rate σ, the angle φ between the rolling direction $\boldsymbol{e}_1$ and $\boldsymbol{e}_\alpha$, and the complementary spin speed ω_3' . Hence the problem of inverse kinematics is to obtain the joint rates $\dot{\eta}_1$ to $\dot{\eta}_n$ and the aforementioned three terms from rolling contact, given the twist of the object $\boldsymbol{S}_{\text{obj}}$.

Suppose the rolling direction is along the vector $\boldsymbol{e}_1$, which makes an angle φ with the vector $\boldsymbol{e}_\alpha$, as in Fig. 2. The vectors $\boldsymbol{e}_1$ and$\boldsymbol{e}_2$ can be expressed in the frame (M-$\boldsymbol{e}_u\boldsymbol{e}_v\boldsymbol{e}_3$) as

$$\begin{aligned} \boldsymbol{e}_1 &= \cos(\theta+\varphi)\,\mathbf{e}_u + \sin(\theta+\varphi)\,\boldsymbol{e}_v \\ \boldsymbol{e}_2 &= -\sin(\theta+\varphi)\,\mathbf{e}_u + \cos(\theta+\varphi)\,\boldsymbol{e}_v \end{aligned} \tag{14}$$

The normal curvature k_n, geodesic curvature k_g, and the geodesic torsion τ_g in the direction of $\boldsymbol{e}_1$ can be obtained in terms of the curvatures of the coordinate curves $\boldsymbol{e}_u$ and $\boldsymbol{e}_v^{21}$ as

$$\begin{aligned} k_n &= k_{nu}\cos^2(\theta+\varphi) + \tau_{gu}\sin 2(\theta+\varphi) + k_{nv}\sin^2(\theta+\varphi) \\ \tau_g &= \tau_{gu}\cos 2(\theta+\varphi) + \tfrac{1}{2}(k_{nv}-k_{nu})\sin 2(\theta+\varphi) \\ k_g &= k_{gu}\cos(\theta+\varphi) + k_{gv}\sin(\theta+\varphi) + \tfrac{\omega'_3}{\sigma} \end{aligned} \tag{15}$$

The coordinates of the contact point M and the curvatures of the coordinate u-, v-, α-, and β-curves at the point M are known. It follows from Eq. (10) that

$$\boldsymbol{\omega}_M = F_1\boldsymbol{e}_u + F_2\boldsymbol{e}_v + F_3\boldsymbol{e}_3 \tag{16}$$

where

$$\begin{aligned} F_1 &= -\tfrac{\sigma}{2}\left((k_{nu}-k_{nv})\sin 3(\theta+\varphi) + (k_{nu}+k_{nv})\sin(\theta+\varphi) + 2\tau_{gu}\cos(\theta+\varphi)\right) \\ F_2 &= \tfrac{\sigma}{2}\left((k_{nu}-k_{nv})\cos 3(\theta+\varphi) + (k_{nu}+k_{nv})\cos(\theta+\varphi) + 2\tau_{gu}\sin(\theta+\varphi)\right) \\ F_3 &= -\sigma\left(k_{gu}\cos(\theta+\varphi) + k_{gv}\sin(\theta+\varphi)\right) - \omega'_3 \end{aligned}$$

Hence, the twist $\boldsymbol{S}_{TM}$ of the frame (M-$\boldsymbol{e}_1\boldsymbol{e}_2\boldsymbol{e}_3$) with respect to the frame (T-$i'j'k'$) can be obtained as

$$\boldsymbol{S}_{TM} = \begin{bmatrix} \boldsymbol{M}\times\boldsymbol{\omega}_M \\ \boldsymbol{\omega}_M \end{bmatrix} \tag{17}$$

The angular velocity of the object frame (O-$i''j''k''$) with respect to the frame (M-$\boldsymbol{e}_1\boldsymbol{e}_2\boldsymbol{e}_3$) is

$$\boldsymbol{\omega}_O = \omega_1\boldsymbol{e}_u + \omega_2\boldsymbol{e}_v + \omega_3\boldsymbol{e}_3 \tag{18}$$

where the parameter ω_i, $i = 1, 2, 3$ can be found in Appendix A. The twist $\boldsymbol{S}_{MO}$ can be obtained as

$$\boldsymbol{S}_{MO} = \begin{bmatrix} \boldsymbol{O}\times\boldsymbol{\omega}_O \\ \boldsymbol{\omega}_O \end{bmatrix} \tag{19}$$

where $\boldsymbol{O}$ represents the position vector MO with respect to the frame (M-$\boldsymbol{e}_1\boldsymbol{e}_2\boldsymbol{e}_3$).

It follows from Eq. (13) that the inverse kinematics is now formulated as system of six nonlinear algebraic equations:

$$\mathbf{J}(\boldsymbol{\eta})\,\dot{\boldsymbol{\eta}} + \left[\, f_1\left(\sigma,\varphi,\omega'_3\right)\cdots f_6\left(\sigma,\varphi,\omega'_3\right)\right]^T = \boldsymbol{S}_{\text{obj}} \tag{20}$$

where $f_i(\sigma, \varphi, \omega'_3)$ are the elements yielded by the rolling contact. In these six scalar equations, the number of unknowns is $n+3$, namely the joint rates $\dot{\eta}_1$ to $\dot{\eta}_n$, and the contact parameters σ, φ, ω_3'. Hence, it takes at least three joints on each finger to manipulate an object in a three-dimensional space, with the other three from rolling contact.

The joint rates $\dot{\eta}_1$ to $\dot{\eta}_n$ can be eliminated by taking the reciprocal product on both sides of Eq. (20) by matrix $\mathbf{J}^{\text{R}}$,[47] which consists of the common reciprocal screws of those in $\mathbf{J}(\boldsymbol{\eta})$. A system of

https://doi.org/10.1017/S026357471700008X Published online by Cambridge University Press

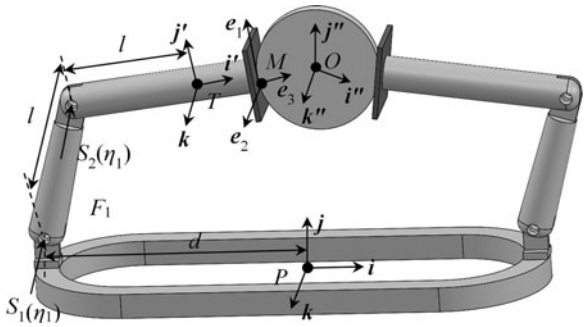

Fig. 3. A planar two-fingered robot hand manipulating a disc.

three nonlinear scalar equations containing the three variables $\sigma, \varphi, \omega'_3$ can be obtained as

$$\mathbf{J}^R \Delta \left[f_1 \left(\sigma, \varphi, \omega'_3\right) \cdots f_6 \left(\sigma, \varphi, \omega'_3\right) \right]^T = \mathbf{J}^R \Delta \boldsymbol{S}_{\text{obj}} \tag{21}$$

where the symbol Δ represents reciprocal product.

4. In-Hand Manipulation of a Planar Two-Fingered Robotic Hand

It suffices to have two joints on each finger for a two-fingered robot to manipulate a disc of unit radius. Set up a palm frame (*P-ijk*), a tool frame (*T-i′j′k′*), a Darboux frame (M-$\boldsymbol{e}_1\boldsymbol{e}_2\boldsymbol{e}_3$), and an object frame (*O-i″j″k″*), as in Fig. 3. Suppose that the origin of the palm frame (*P-ijk*) to the first joint of each finger is d, and the length of each fingerer section is l. The contact locus on the end-effector of the finger F_1 is a straight line along the $\boldsymbol{e}_1$-axis, and the contact locus on the object (disc) is a circle of radius R.

4.1. Forward kinematics

The frame (*T-i′j′k′*) on the fingertip with respect to the frame (*P-ijk*) can be obtained by the product of exponentials formula in joint-space as

$$\boldsymbol{g}_{PT} = e^{S_1 \eta_1} e^{S_2 \eta_2} \boldsymbol{g}_{PT}(0) = \begin{bmatrix} \mathrm{c}\eta_{12} & -\mathrm{s}\eta_{12} & 0 & l\left(\mathrm{c}\eta_1 + \mathrm{c}\eta_{12}\right) - d \\ \mathrm{s}\eta_{12} & \mathrm{c}\eta_{12} & 0 & l\left(\mathrm{s}\eta_1 + \mathrm{s}\eta_{12}\right) \\ 0 & 0 & 1 & 0 \\ 0 & 0 & 0 & 1 \end{bmatrix} \tag{22}$$

where c represents cosine and s represents sine, $\eta_{12} = \eta_1 + \eta_2$, and $\eta_{123} = \eta_1 + \eta_2 + \eta_3$. It follows from Eq. (2) the twist $\boldsymbol{S}_{PT}$ is

$$\boldsymbol{S}_{PT} = \begin{bmatrix} l\dot{\eta}_2 \mathrm{s}\eta_1 \\ d\dot{\eta}_1 + \dot{\eta}_2\left(d - l\mathrm{s}\eta_1\right) \\ 0 \\ 0 \\ 0 \\ \dot{\eta}_{12} \end{bmatrix} \tag{23}$$

https://doi.org/10.1017/S026357471700008X Published online by Cambridge University Press

The homogeneous transformation matrix of the frame (M-$\boldsymbol{e}_1\boldsymbol{e}_2\boldsymbol{e}_3$) with respect to the frame (T-$i'j'k'$) is

$$\boldsymbol{g}_{TM} = \begin{bmatrix} 0 & 0 & 1 & M_x \\ 1 & 0 & 0 & M_y \\ 0 & 1 & 0 & 0 \\ 0 & 0 & 0 & 1 \end{bmatrix} \tag{24}$$

where M_x and M_y are the coordinates of the contact point M. The contact locus L on the fingertip is a straight line, thus the geodesic curvature k_g, normal curvature k_n, and the geodesic torsion τ_g are 0. The twist $\boldsymbol{S}_{TM}$ can be obtained from Eq. (9) as

$$\boldsymbol{S}_{TM} = \begin{bmatrix} 0 & 0 & 0 & 0 & 0 & 0 \end{bmatrix}^T \tag{25}$$

On the contact locus L', the geodesic curvature k_g' and the geodesic torsion τ_g' are 0, and the normal curvature k_n' is $1/R$. It follows from Eq. (11) that the angular velocity of the disc frame (O-$i''j''k''$) with respect to the frame (M-$\boldsymbol{e}_1\boldsymbol{e}_2\boldsymbol{e}_3$) is

$$\boldsymbol{\omega}_O = \frac{\sigma \boldsymbol{e}_2}{R} \tag{26}$$

The twist of the disc frame (O-$i''j''k''$) with respect to the frame (M-$\boldsymbol{e}_1\boldsymbol{e}_2\boldsymbol{e}_3$) from Eq. (12) is as follows:

$$\boldsymbol{S}_{MO} = \begin{bmatrix} \boldsymbol{O} \times \frac{\sigma \boldsymbol{e}_2}{R} \\ \frac{\sigma \boldsymbol{e}_2}{R} \end{bmatrix} = \begin{bmatrix} -\sigma \\ 0 \\ 0 \\ 0 \\ \frac{\sigma}{R} \\ 0 \end{bmatrix} \tag{27}$$

where the coordinates of the point $\boldsymbol{O}$ with respect to the frame (M-$\boldsymbol{e}_1\boldsymbol{e}_2\boldsymbol{e}_3$) are $[0\ 0\ R]^T$. It follows from Eq. (13) the twist of the object frame (O-$i''j''k''$) with respect to the palm frame (P-ijk) is

$$\boldsymbol{S}_{PO} = \begin{bmatrix} A_1 & A_2 & 0 & 0 & 0 & A_3 \end{bmatrix}^T \tag{28}$$

where

$$\begin{aligned} A_1 &= l\dot{\eta}_2 \mathrm{s}\eta_1 + \tfrac{\sigma}{R}\left(M_y \mathrm{c}\eta_{12} + M_x \mathrm{s}\eta_{12} + l\mathrm{s}\eta_{12} + l\mathrm{s}\eta_1 + R\mathrm{s}\eta_{12}\right) \\ A_2 &= \dot{\eta}_1 d + \dot{\eta}_2 (d - l\mathrm{c}\eta_1) + \tfrac{\sigma}{R}\left(-d - M_x \mathrm{c}\eta_{12} - M_y \mathrm{s}\eta_{12} + l\mathrm{c}\eta_{12} + l\mathrm{c}\eta_1 - R\mathrm{c}\eta_{12}\right) \\ A_3 &= \dot{\eta}_{12} + \tfrac{\sigma}{R} \end{aligned}$$

This completes the forward kinematics.

4.2. Inverse kinematics

For inverse kinematics, the angular velocity is given at a certain configuration. Suppose the angular velocity of the disc is ω when the centre O of the disc is at (O_x, O_y) at time t. The twist of the disc is

$${}^P\boldsymbol{S}_{PO} = \begin{bmatrix} O_y\omega, & -O_x\omega & 0 & 0 & 0 & \omega \end{bmatrix}^T \tag{29}$$

In this example, the contact locus on the end-effector is a straight line and the contact locus on the object is the outer circle of the disc. Hence, the inverse problem is reduced to equating the elements

https://doi.org/10.1017/S026357471700008X Published online by Cambridge University Press

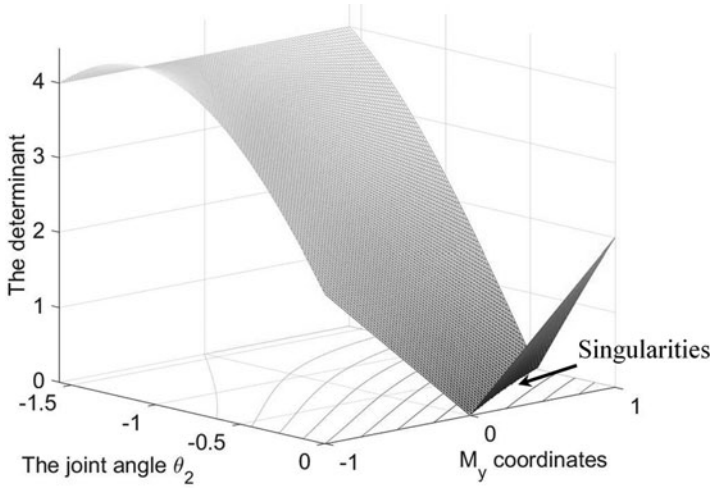

Fig. 4. Singularities in an augmented joint space.

in Eq. (28) to the corresponding elements in Eq. (29). This generates a system of linear equations for the inverse kinematics:

$$\begin{bmatrix} 0 & l\mathrm{s}\eta_1 & \frac{1}{R}\left(M_y\mathrm{c}\eta_{12} + M_x\mathrm{s}\eta_{12} + l\mathrm{s}\eta_{12} + l\mathrm{s}\eta_1 + R\mathrm{s}\eta_{12}\right) \\ d & d - l\mathrm{c}\eta_1 & \frac{1}{R}\left(-d - M_x\mathrm{c}\eta_{12} - M_y\mathrm{s}\eta_{12} + l\mathrm{c}\eta_{12} + l\mathrm{c}\eta_1 - R\mathrm{c}\eta_{12}\right) \\ 1 & 1 & \frac{1}{R} \end{bmatrix} \begin{bmatrix} \dot{\eta}_1 \\ \dot{\eta}_2 \\ \sigma \end{bmatrix} = \begin{bmatrix} O_y\omega \\ -O_x\omega \\ \omega \end{bmatrix} \quad (30)$$

The variables $\dot{\eta}_1, \dot{\eta}_2, \sigma$ can be obtained straightforwardly.

4.3. Singularities

Singularities occur when the determinate of the matrix in Eq. (30) is 0. The closed-form determinant can be obtained as

$$\det(\mathbf{A}) = \frac{a}{R}\left(M_y\cos\eta_2 + M_x\sin\eta_2 + R\sin\eta_2 + l\sin\eta_2\right) \quad (31)$$

Suppose $l = 1$, $M_x = l/2 = 1/2$, M_y in the range of $[-1/2, 1/2]$, η_2 in the range of $[-\pi/2, 0]$. In this example, it can be found that the combinations of the joint angle η_2 and M_y yield singularities at certain configurations, as in Fig. 4.

To the best of the authors' knowledge, it is the first time that the singularities caused by the positions of the contact point are discovered.

5. In-Hand Manipulation of the Three-Fingered MetaHand

The MetaHand[48] is used in the case study, where the palm is simplified to a rigid ring. Set up a palm frame (P-ijk), a tool frame (T-$i'j'k'$), a Darboux frame (M-$\boldsymbol{e}_1\boldsymbol{e}_2\boldsymbol{e}_3$), and an object frame ($O$-$i''j''k''$), as in Fig. 5. Suppose that the origin of the palm frame P to the first joint of each finger is d, and the length of each fingerer section is l.

The fingertip is a hemi-ellipsoid, which can be parameterized as

$$\begin{gathered} \boldsymbol{r}_1(u, v) = \begin{bmatrix} b_1\cos v & a_1\sin v\cos u & a_1\sin v\sin u \end{bmatrix}^T \\ u \in [0, 2\pi),\ v \in \left[0, \tfrac{\pi}{2}\right) \end{gathered} \quad (32)$$

https://doi.org/10.1017/S026357471700008X Published online by Cambridge University Press

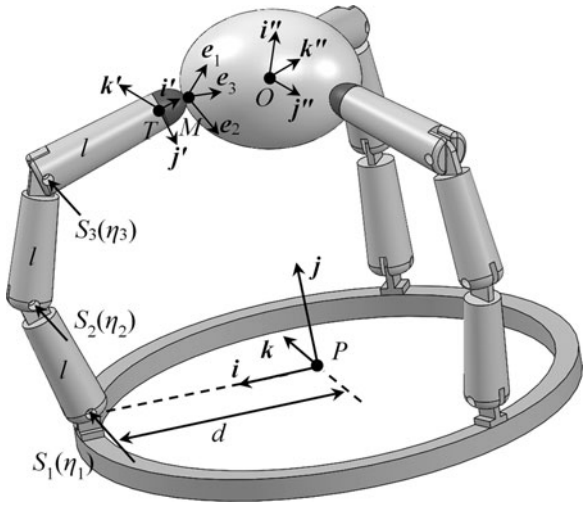

Fig. 5. Three-fingered robot hand manipulating an ellipsoid object.

The object is an ellipsoid, which can be parameterized as

$$\begin{gathered} \boldsymbol{r}_2(\alpha, \beta) = \begin{bmatrix} b_2 \mathrm{cos}\beta & a_2 \mathrm{sin}\beta \mathrm{cos}\alpha & a_2 \sin\beta \sin\alpha \end{bmatrix}^T \\ \alpha \in \begin{bmatrix} 0 & 2\pi \end{bmatrix}, \beta \in [0, \pi) \end{gathered} \tag{33}$$

5.1. Forward kinematics

The frame (*T-i'j'k'*) on the fingertip with respect to the frame (*P-ijk*) can be obtained by the product of exponentials formula in joint-space as

$$\boldsymbol{g}_{PT} = e^{S_1\eta_1} e^{S_2\eta_2} e^{S_3\eta_3} \boldsymbol{g}_{PT}(0) = \begin{bmatrix} \mathrm{c}\eta_{123} & -\mathrm{s}\eta_{123} & 0 & l(\mathrm{c}\eta_1 + \mathrm{c}\eta_{12} + \mathrm{c}\eta_{123}) + d \\ \mathrm{s}\eta_{123} & \mathrm{c}\eta_{123} & 0 & l(\mathrm{s}\eta_1 + \mathrm{s}\eta_{12} + \mathrm{s}\eta_{123}) \\ 0 & 0 & 1 & 0 \\ 0 & 0 & 0 & 1 \end{bmatrix} \tag{34}$$

where c represents cosine and s represents sine, $\eta_{12} = \eta_1 + \eta_2$, and $\eta_{123} = \eta_1 + \eta_2 + \eta_3$. It follows from Eq. (2) the twist $\boldsymbol{S}_{PT}$ is

$$\boldsymbol{S}_{PT} = \begin{bmatrix} l(\dot{\eta}_2 \mathrm{s}\eta_1 + \dot{\eta}_3(\mathrm{s}\eta_1 + \mathrm{s}\eta_{12})) \\ -d\dot{\eta}_1 - \dot{\eta}_2(d + l\mathrm{c}\eta_1) - \dot{\eta}_3(d + l\mathrm{c}\eta_1 + l\mathrm{c}\eta_{12}) \\ 0 \\ 0 \\ 0 \\ \dot{\eta}_{123} \end{bmatrix} \tag{35}$$

Suppose the contact locus L on the fingertip is a v-coordinate curve, which is circle, and the contact locus L' on the ellipsoidal object is an α-coordinate curve, which is an ellipse. Set up the Darboux frame (M-$\boldsymbol{e}_1\boldsymbol{e}_2\boldsymbol{e}_3$) at the contact point M, where $\boldsymbol{e}_1$ is the common unit tangent vector along L and L', $\boldsymbol{e}_3$ is the common normal vector of the two surfaces, as in Fig. 6.

https://doi.org/10.1017/S026357471700008X Published online by Cambridge University Press

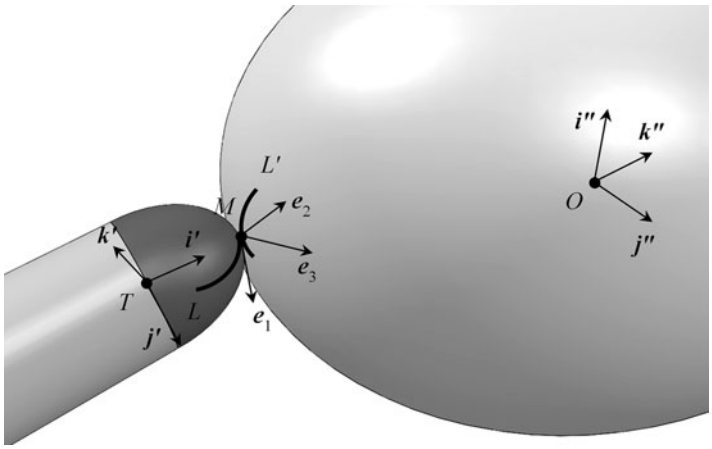

Fig. 6. The contact locus L on the fingertip and L' on the object.

The unit vectors $\boldsymbol{e}_1$, $\boldsymbol{e}_2$, and $\boldsymbol{e}3$ with respect to the frame (T-$i'j'k'$) are, respectively,

$$\begin{aligned}
\boldsymbol{e}_1 &= \tfrac{1}{D}\begin{bmatrix} -b_1 \sin v & a_1 \cos u \cos v & a_1 \sin u \cos v \end{bmatrix} \\
\boldsymbol{e}_2 &= \begin{bmatrix} 0 & \sin u & -\cos u \end{bmatrix} \\
\boldsymbol{e}_3 &= \tfrac{1}{D}\begin{bmatrix} -a_1 \cos v & -b_1 \cos u \sin v & -b_1 \sin u \sin v \end{bmatrix}
\end{aligned} \tag{36}$$

where $D_1 = \sqrt{a_1^2 \cos^2 v + b_1^2 \sin^2 v}$. The normal curvature k_n, geodesic torsion τ_g, and geodesic curvature k_g in the direction of $\boldsymbol{e}_1$ at the point M of the fingertip are, respectively,

$$k_n = \frac{-a_1 b_1}{D_1^3}, \quad k_g = 0, \quad \tau_g = 0 \tag{37}$$

The angular velocity of the frame (M-$\boldsymbol{e}_1\boldsymbol{e}_2\boldsymbol{e}_3$) with respect to the frame (T-$i'j'k'$) is

$$\boldsymbol{\omega}_M = \sigma\left(-\tau_g \boldsymbol{e}_1 + k_n \boldsymbol{e}_2 - k_g \boldsymbol{e}_3\right) = \frac{-\sigma a_1 b_1}{D_1^3}\boldsymbol{e}_2 \tag{38}$$

It follows that the twist of the frame (M-$\boldsymbol{e}_1\boldsymbol{e}_2\boldsymbol{e}_3$) with respect to the frame (T-$i'j'k'$) is

$$\boldsymbol{S}_{TM} = \begin{bmatrix} \boldsymbol{TM} \times \boldsymbol{\omega}_M \\ \boldsymbol{\omega}_M \end{bmatrix} = \frac{\sigma}{D}\begin{bmatrix} \frac{a_1^2 b_1 \sin v}{D^2} \\ -a_1 b_1^2 \cos u \cos v \\ -a_1 b_1^2 \sin u \cos v \\ 0 \\ -a_1 b_1 \sin u \\ a_1 b_1 \cos u \end{bmatrix} \tag{39}$$

where $\boldsymbol{TM} = [\, b_1 \cos v \quad a_1 \sin v \cos u \quad a_1 \sin v \sin u \,]^T$.

The normal curvature k_n' , geodesic torsion τ_g' , and geodesic curvature k_g' in the direction of $\boldsymbol{e}_1$ at the point M of the object are, respectively,

$$k_n' = \frac{-a_2 b_2}{{D_2}^3}, \quad k_g' = 0, \quad \tau_g' = 0 \tag{40}$$

https://doi.org/10.1017/S026357471700008X Published online by Cambridge University Press

where $D_2 = \sqrt{a_2^2 \cos^2\beta + b_2^2 \sin^2\beta}$. It follows from Eq. (11) that the angular velocity of the object frame (O-$i''j''k''$) with respect to the frame (M-$\boldsymbol{e}_1\boldsymbol{e}_2\boldsymbol{e}_3$) is

$$\boldsymbol{\omega}_O = \sigma\left(\left(\tau'_g - \tau_g\right)\boldsymbol{e}_1 + \left(k'_n - k_n\right)\boldsymbol{e}_2 + \left(k'_g - k_g\right)\boldsymbol{e}_3\right) = \sigma\left(-\frac{a_2 b_2}{D_2^3} + \frac{a_1 b_1}{D_1^3}\right)\boldsymbol{e}_2 \tag{41}$$

It follows the twist of the object frame (O-$i''j''k''$) with respect to the frame (M-$\boldsymbol{e}_1\boldsymbol{e}_2\boldsymbol{e}_3$) is

$$\boldsymbol{S}_O = \begin{bmatrix} \boldsymbol{MO} \times \boldsymbol{\omega}_O \\ \boldsymbol{\omega}_O \end{bmatrix} = \sigma \begin{bmatrix} -a_2^2 b_2\left(\dfrac{a_2 b_2}{D_2^3} + \dfrac{a_1 b_1}{D_1^3}\right) \\ 0 \\ 0 \\ 0 \\ -\dfrac{a_2 b_2}{D_2^3} - \dfrac{a_1 b_1}{D_1^3} \\ 0 \end{bmatrix} \tag{42}$$

where $\boldsymbol{MO} = \dfrac{1}{D_2^2}(\sin\beta\cos\beta(a_2^2 - b_2^2)\boldsymbol{e}_2 - a_2 b_2 \boldsymbol{e}_3)$.

The twist of the object frame (O-$i''j''k''$) with respect to the palm frame (P-ijk) can be obtained straightforwardly from Eq. (13).

5.2. Inverse kinematics

A numerical example was used to illustrate the proposed approach, since inverse kinematics of in-hand manipulation does not admit closed-form solutions in general cases.

Suppose the desired twist of the unit ball is $\boldsymbol{S}_{\text{obj}} = [2\ -0.5\ -1.5\ 1\ 1\ 1]^T$ and the structural parameters are: $d = 1.5$, $l = 1$, $a = 0.2$, $b = 0.15$. The robot hand is in the following configuration:

$$\begin{aligned} &\eta_1 = \frac{\pi}{3}, \quad \eta_2 = \frac{\pi}{3}, \quad \eta_3 = \frac{\pi}{6} \\ &u_0 = \frac{\pi}{4}, \quad v_0 = \frac{3\pi}{4} \\ &\alpha_0 = \frac{\pi}{4}, \quad \beta_0 = \frac{\pi}{4} \end{aligned}$$

It follows from Eq. (2) that the homogeneous transformation matrix $\boldsymbol{g}_{PT}$ is

$$\boldsymbol{g}_{PT} = \begin{bmatrix} -0.5 & -0.866 & 0 & 0.634 \\ 0.866 & -0.5 & 0 & 2.232 \\ 0 & 0 & 1 & 0 \\ 0 & 0 & 0 & 1 \end{bmatrix}$$

https://doi.org/10.1017/S026357471700008X Published online by Cambridge University Press

And the finger joint Jacobian is

$$\mathbf{J}(\boldsymbol{\eta}) = \begin{bmatrix} 0 & 0.866 & 1.732 \\ -1.5 & -2.0 & -1.5 \\ 0 & 0 & 0 \\ 0 & 0 & 0 \\ 0 & 0 & 0 \\ 1 & 1 & 1 \end{bmatrix}$$

The coordinates of the contact point M with respect to the frame (T-$i'j'k'$) is $\boldsymbol{M} = [0.106, 0.10, 0.10]^T$, and the unit tangent vectors $\boldsymbol{e}_u$ and $\boldsymbol{e}_v$ of the coordinate curves and the normal vector $\boldsymbol{e}_3$ of the fingertip ellipsoid at the contact point M are, respectively,

$$\begin{aligned} \boldsymbol{e}_u &= \begin{bmatrix} 0 & -0.71 & 0.71 \end{bmatrix}^T \\ \boldsymbol{e}_v &= \begin{bmatrix} -0.6 & 0.57 & 0.57 \end{bmatrix}^T \\ \boldsymbol{e}_3 &= \begin{bmatrix} -0.8 & -0.42 & -0.42 \end{bmatrix}^T \end{aligned} \tag{43}$$

On the fingertip ellipsoid, the normal curvature, geodesic torsion, and geodesic curvature at the point M in the direction of $\boldsymbol{e}_u$ and $\boldsymbol{e}_v$ can be obtained[21] as

$$k_{nu} = -4.243, k_{nv} = -5.431, k_{gu} = -5.657, k_{gv} = 0, \tau_{gu} = \tau_{gv} = 0 \tag{44}$$

The unit tangent vector $\boldsymbol{e}_\alpha$ and $\boldsymbol{e}_\beta$ of the unit ball at the contact point M are, respectively,

$$\begin{aligned} \boldsymbol{e}_\alpha &= \begin{bmatrix} 0 & -0.866 & 0.5 \end{bmatrix}^T \\ \boldsymbol{e}_\beta &= \begin{bmatrix} -0.756 & 0.327 & 0.567 \end{bmatrix}^T \end{aligned}$$

On the unit ball, the normal curvature, geodesic torsion, and geodesic curvature at the point M in the direction of $\boldsymbol{e}_\alpha$ and $\boldsymbol{e}_\beta$ can be obtained[21] as

$$k_{n\alpha} = 1.455, k_{n\beta} = 2.493, k_{g\alpha} = -1.26, k_{g\beta} = 0, \tau_{g\alpha} = \tau_{g\beta} = 0 \tag{45}$$

The angle θ between $\boldsymbol{e}_u$ and $\boldsymbol{e}_\alpha$ is 0.268 rad. The unit vector $\boldsymbol{e}_1$ along the desired rolling direction can be obtained from Eq. (14) as

$$\begin{aligned} \boldsymbol{e}_1 &= \begin{bmatrix} -0.6\sin(\varphi + 0.262) \\ -0.707\cos(\varphi + 0.262) + 0.566\sin(\varphi + 0.262) \\ 0.707\cos(\varphi + 0.262) + 0.566\sin(\varphi + 0.262) \end{bmatrix}^T, \\ \boldsymbol{e}_2 &= \begin{bmatrix} -0.6\cos(\varphi + 0.262) \\ 0.707\sin(\varphi + 0.262) + 0.566\cos(\varphi + 0.262) \\ -0.707\sin(\varphi + 0.262) + 0.566\cos(\varphi + 0.262) \end{bmatrix}^T \end{aligned} \tag{46}$$

The unit normal vector $\boldsymbol{e}_3$ has been obtained in Eq. (43). The homogeneous transformation matrix from the frame (T-$i'j'k'$) to the frame (M-$\boldsymbol{e}_1\boldsymbol{e}_2\boldsymbol{e}_3$) is

$$\boldsymbol{g}_{TM} = \begin{bmatrix} \boldsymbol{e}_1^T & \boldsymbol{e}_2^T & \boldsymbol{e}_3^T & M \\ 0 & 0 & 0 & 1 \end{bmatrix} \tag{47}$$

https://doi.org/10.1017/S026357471700008X Published online by Cambridge University Press

It follows from Eq. (16) the angular velocity of the frame (M-$\boldsymbol{e}_1\boldsymbol{e}_2\boldsymbol{e}_3$) in terms of the rolling rate σ, rolling direction φ, and the compensatory spin rate ω_3' is

$$\boldsymbol{\omega}_M = \begin{bmatrix} \sigma\left(-1.008\cos^3\varphi + 1.008\cos^2\varphi\sin\varphi + 0.168\sin\varphi - 0.812\cos\varphi\right) + 0.8\omega' \\ \sigma\left(2.138\cos^3\varphi + 0.238\cos^2\varphi\sin\varphi - 2.034\sin\varphi - 7.45\cos\varphi\right) + 0.424\omega' \\ \sigma\left(-0.238\cos^3\varphi - 2.138\cos^2\varphi\sin\varphi - 3.898\cos\varphi + 5.167\sin\varphi\right) + 0.424\omega' \end{bmatrix} \tag{48}$$

The twist $\boldsymbol{S}_{TM}$ of the frame (M-$\boldsymbol{e}_1\boldsymbol{e}_2\boldsymbol{e}_3$) with respect to the frame (T-$i'j'k'$) can be obtained as

$$\boldsymbol{S}_{TM} = \begin{bmatrix} \boldsymbol{M} \times \boldsymbol{\omega}_M \\ \boldsymbol{\omega}_M \end{bmatrix} \tag{49}$$

where $\boldsymbol{M} = [0.106, 0.10, 0.10]^T$. It follows from Eq. (18) that the angular velocity of the object frame (O-$i''j''k''$) with respect to the frame (M-$\boldsymbol{e}_1\boldsymbol{e}_2\boldsymbol{e}_3$) is

$$\boldsymbol{\omega}_O = \begin{bmatrix} -\sigma\left(-1.68\cos^3\varphi - 1.68\cos^2\varphi\sin\varphi + 7.501\sin\varphi + 2.888\cos\varphi\right) \\ \sigma\left(-1.68\cos^3\varphi + 1.68\cos^2\varphi\sin\varphi - 2.317\sin\varphi + 7.337\cos\varphi\right) \\ \sigma\left(-1.464\sin\varphi + 4.204\cos\varphi\right) + \omega' \end{bmatrix} \tag{50}$$

The coordinates of the centre O of the ellipsoid respect to the frame (M-$\boldsymbol{e}_1\boldsymbol{e}_2\boldsymbol{e}_3$) is

$$O = \begin{bmatrix} -0.282\sin(\varphi + 0.262) \\ 0.1345\sin(\varphi + 0.262) \\ 0.4611 \end{bmatrix} \tag{51}$$

Hence, the twist $\boldsymbol{S}_{MO}$ of the frame (O-$i''j''k''$) with respect to the frame (M-$\boldsymbol{e}_1\boldsymbol{e}_2\boldsymbol{e}_3$) is

$$\boldsymbol{S}_{MO} = \begin{bmatrix} \mathbf{O} \times \boldsymbol{\omega}_O \\ \boldsymbol{\omega}_O \end{bmatrix} \tag{52}$$

It follows from Eq. (20) that the inverse kinematics in terms of the joint rates $\dot{\eta}_1$, $\dot{\eta}_2$, $\dot{\eta}_3$ and the rolling rate, rolling direction, and the compensatory spin rate σ, φ, ω_3' is

$$\begin{bmatrix} 0 & 0.866 & 1.732 \\ -1.5 & -2.0 & -1.5 \\ 0 & 0 & 0 \\ 0 & 0 & 0 \\ 0 & 0 & 0 \\ 1 & 1 & 1 \end{bmatrix} \begin{bmatrix} \dot{\eta}_1 \\ \dot{\eta}_2 \\ \dot{\eta}_3 \end{bmatrix} + \begin{bmatrix} f_1\left(\sigma, \varphi, \omega'_3\right) \\ f_2\left(\sigma, \varphi, \omega'_3\right) \\ f_3\left(\sigma, \varphi, \omega'_3\right) \\ f_4\left(\sigma, \varphi, \omega'_3\right) \\ f_5\left(\sigma, \varphi, \omega'_3\right) \\ f_6\left(\sigma, \varphi, \omega'_3\right) \end{bmatrix} = \boldsymbol{S}_{\text{Obj}} \tag{53}$$

where $f_1(\sigma, \varphi, \omega'_3)$ to $f_6(\sigma, \varphi, \omega'_3)$ can be found in Appendix B.

Let $\mathbf{J}^R$ represent the reciprocal matrix of $\mathbf{J}$, and taking the reciprocal product on the both sides of Eq. (53) eliminates the joint rates $\dot{\eta}_1$, $\dot{\eta}_2$, $\dot{\eta}_3$, yielding three nonlinear algebraic equations in terms of

https://doi.org/10.1017/S026357471700008X Published online by Cambridge University Press

$\sigma, \varphi, \omega'_3$:

$$\begin{aligned}
&\sigma\begin{pmatrix}-0.207+0.385\cos^2\varphi-0.196\cos^3\varphi+0.624\cos\varphi+2.196\sin\varphi\\+0.112\cos 3\varphi\cos\varphi+0.227\cos 3\varphi\sin\varphi+0.227\sin 3\varphi\cos\varphi-0.112\sin 3\varphi\sin\varphi\\-5.783\cos\varphi\sin\varphi-0.992\cos^2\varphi\sin\varphi\end{pmatrix}=1\\
&\sigma\begin{pmatrix}7.259+13.49\cos^2\varphi-2.356\cos^3\varphi+6.183\cos\varphi+1.798\sin\varphi\\+0.550\cos 3\varphi\cos\varphi-0.225\cos 3\varphi\sin\varphi-0.225\sin 3\varphi\cos\varphi-0.550\sin 3\varphi\sin\varphi\\-1.844\cos\varphi\sin\varphi+0.298\cos^2\varphi\sin\varphi\end{pmatrix}=1\\
&\sigma\begin{pmatrix}-0.683+13.11\cos^2\varphi+1.943\cos^3\varphi+2.002\sin^3\varphi-0.419\cos 2\varphi\\+0.039\cos 4\varphi-5.722\sin 2\varphi+0.003\sin 4\varphi-3.483\cos\varphi\\+1.839\sin\varphi-0.256\cos 3\varphi\cos\varphi+0.699\cos 3\varphi\sin\varphi+0.699\sin 3\varphi\cos\varphi\\+0.256\sin 3\varphi\sin\varphi\end{pmatrix}\\
&+\omega'_3\left(0.178-0.079\sin 2\varphi-0.234\cos^2\varphi\right)=1.5
\end{aligned} \tag{54}$$

The rolling rate σ can be eliminated from the first two equations in Eq. (54), yielding a trigonometric equation containing only the rolling angle φ. The half-angle formulas $\sin\varphi = 2x/(1+x^2)$, $\cos\varphi = (1-x^2)/(1+x^2)$, where $x = \tan(\varphi/2)$, can be used to transform this trigonometric equation to a polynomial of degree eight:

$$\begin{aligned}
&9.37x^8+2.484x^7-2.158x^6+38.12x^5-103.2x^4\\
&-28.18x^3-33.03x^2-6.052x+2.572=0
\end{aligned} \tag{55}$$

Of the eight roots of this polynomial, the four real roots are

$$x_1=-2.193,\ x_2=1.632,\ x_3=-0.353,\ x_4=0.186 \tag{56}$$

Substituting these roots into the first equation in Eq. (54) yields the four rolling rates σ as

$$\sigma_1=-0.210,\ \sigma_2=0.256,\ \sigma_3=0.488,\ \sigma_4=-1.484 \tag{57}$$

Since the rolling rate cannot be negative, σ_1 and σ_4 are discarded. Substituting the two sets left into the third equation in Eq. (54) yields the compensatory spin rate ω'_3 as

$$\omega'_{31}=-0.116,\ \omega'_{32}=0.017 \tag{58}$$

The two sets $(\varphi=2.042, \sigma=0.256, \omega'_3=-0.1022)$, $(\varphi=-0.679, \sigma=0.488, \omega'_3=1.0591)$ can be substituted into Eq. (53) to yield the joint rates as

$$\begin{aligned}
&(\eta_1=0.1604, \eta_2=1.1265, \eta_3=-2.6857)\\
&(\eta_1=1.2230, \eta_2=-1.9444, \eta_3=0.8709)
\end{aligned} \tag{59}$$

This completes the inverse kinematics.

6. Results and Discussions

This paper does not discuss dynamic analysis of in-hand manipulation with rolling contact for the following reasons. Robotic hands in general operate at low speeds and low accelerations, where inertial forces are negligible.[49] Hence, dynamic analysis of in-hand manipulation can be treated as quasi-static analysis,[50,51] where the wrenches generated by rolling contact, which is termed point contact with friction, include one along the common normal vector and two parallel to the tangent

https://doi.org/10.1017/S026357471700008X Published online by Cambridge University Press

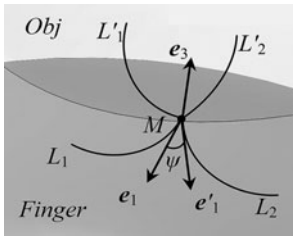

Fig. 7. Piecewise smooth contact trajectories.

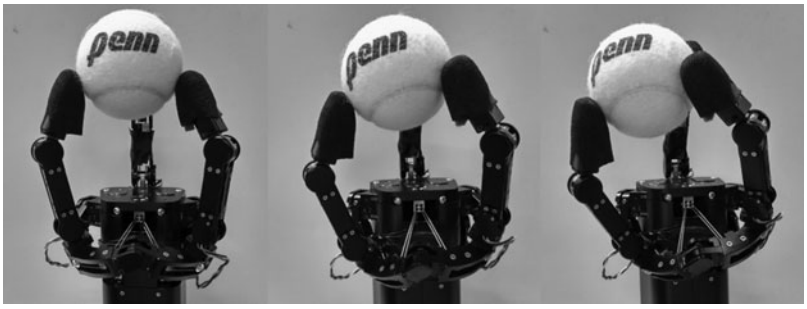

Fig. 8. The MetaHand rotating a tennis ball.

plane.[33] An in-depth study of quasi-static analysis of multifingered hands has been extensively investigated, for example ref. [33, 36, 50, 51] and is not repeated here.

Contact trajectories can be piecewise smooth curve with discontinuous tangent vectors, where L_1 and L_2 are the contact trajectories on the fingertip. At the point M, where the discontinuity occurs, the tangent vector $\boldsymbol{e}_1$ of L_1 and the tangent vector $\boldsymbol{e}'_1$ of L_2 make an angle ψ, as in Fig. 7.

Assume at time $t = t_0$ the finger stops rolling the object along the trajectory L_1 and starts to roll the object along the L_2. To apply the proposed approach, the moving frame from (M-$\boldsymbol{e}_1\boldsymbol{e}_2\boldsymbol{e}_3$) can be replaced to ($M$-$\boldsymbol{e}'_1\boldsymbol{e}'_2\boldsymbol{e}_3$) and use the curvatures of L_2 and L'_2 after $t = t_0$, where $\boldsymbol{e}_3$ remains unchanged and $\boldsymbol{e}'_1 = \cos\psi\, \boldsymbol{e}_1 + \sin\psi \boldsymbol{e}_2$, $\boldsymbol{e}'_2 = -\sin\psi \boldsymbol{e}_1 + \cos\psi \boldsymbol{e}_2$.

The degree of final polynomials for more complex surfaces is still six. This can be seen from the equations in Appendix A, where the parameters A_i, B_i, and C_i are constants. The first step to obtain the rolling direction φ is to eliminate the rolling rate σ by dividing ω_1 by ω_1. This yields a nonlinear trigonometric equation with highest terms, including $\cos^3\varphi$, $\sin^3\varphi$, $\cos^2\varphi \sin\varphi$, and $\sin^2\varphi \cos\varphi$. Substituting the half-tangent-angle $x = \tan\frac{\varphi}{2}$ yields a polynomial of degree six. This is valid for any complex surface.

The proposed approach has been implemented on the MetaHand,[48] which has an articulated palm with three identical fingers attached on it. The palm is formed by a spherical five-bar linkage that can alter its geometry to relocate the fingers to implement in-hand manipulation. Product-of-exponential-based kinematics analysis of the MetaHand and its corresponding grasp constraints analysis during manipulating an object were presented in the literature.[45] A preliminary experiment to verify the rolling contact model based on the Metahand is shown in Fig. 8. More specifically, the three-fingered hand first executes a tripod grasp to catch a tennis ball with its fingertips. Then, the palm is actuated to change its configuration to reposition and reorientate the fingers in such a way that the rolling between the object and fingertips occurs during maintaining the grasp, triggering the in-hand manipulation as a consequence. Hence, the ball changes its location by the three fingers and an articulated palm using rolling contact.

7. Conclusions

We integrated the product of exponential formula and the moving frame method to yield a compact form for the forward kinematics; this laid the foundation of the inverse kinematics, which was formulated as a system of nonlinear algebraic equations in terms of the joint rates of the finger linkage mechanism and the parameters of the contact trajectories. This approach provides an alternative to the

https://doi.org/10.1017/S026357471700008X Published online by Cambridge University Press

existing one that is in the form of a system of nonlinear differential equations. One advantage of the proposed approach is that the nonlinear equations can solved by being transformed into a polynomial that admits reliable and fast root approximation, as demonstrated by a three-fingered robot hand with hemi-ellipsoid fingertips manipulating an ellipsoid object.

Appendix A

$$\omega_1 = \sigma \begin{pmatrix} A_1 \cos^3\varphi + A_2 \sin^3\varphi + A_3 \cos^2\varphi \sin\varphi + \\ A_4 \cos\varphi \sin^2\varphi + A_5 \cos\varphi + A_6 \sin\varphi \end{pmatrix}$$

$$\omega_2 = \sigma \begin{pmatrix} B_1 \cos^3\varphi + B_2 \sin^3\varphi + B_3 \cos^2\varphi \sin\varphi + \\ B_4 \cos\varphi \sin^2\varphi + B_5 \cos\varphi + B_6 \sin\varphi \end{pmatrix}$$

$$\omega_3 = \sigma \left(C_1 \cos\varphi + C_2 \sin\varphi\right) + \omega_3'$$

where

$$\begin{aligned}
A_1 &= -k_{n\alpha} \sin\theta + (-2k_{nv} + 3k_{nu}) \cos^2\theta \sin\theta + 4\tau_{gu} \cos^3\theta \\
&\quad - \left(2\tau_{gu} \cos^2\theta + 2\tau_{g\alpha}\right) \cos\theta + k_{nv} \sin^3\theta \\
A_2 &= -2\tau_{gu} \sin\theta \cos^2\theta + \left(-k_{n\beta} + k_{nu} \sin^2\theta\right) \cos\theta + k_{nv} \cos^3\theta \\
A_3 &= (-2k_{nv} + 3k_{nu}) \cos^3\theta + 2\tau_{gu} \sin\theta - 4\tau_{gu} \sin\theta \cos^2\theta \\
&\quad + \left((5k_{nv} - 4k_{nu}) \sin^2\theta - k_{n\beta} - k_{nu} + k_{nv}\right) \cos\theta - 2\tau_{gu} \sin^3\theta \\
A_4 &= (5k_{nv} - 4k_{nu}) \sin\theta \cos^2\theta + 2\tau_{gu} \cos^3\theta - 2\tau_{g\alpha} \cos\theta \\
&\quad + k_{nu} \sin^3\theta + (k_{nu} - k_{nv} - k_{n\alpha}) \sin\theta \\
A_5 &= \cos\theta \left(-2\tau_{gu} \cos^2\theta + (-k_{nu} + k_{nv}) \sin\theta \cos\theta + \tau_{g\alpha} + \tau_{gu}\right) \\
A_6 &= \sin\theta \left(2\tau_{gu} \cos^2\theta + (k_{nu} - k_{nv}) \sin\theta \cos\theta - \tau_{g\alpha} - \tau_{gu}\right)
\end{aligned}$$

$$\begin{aligned}
B_1 &= k_{n\alpha} \cos\theta + \left(-2\tau_{g\alpha} - 2\tau_{gu} \sin^2\theta\right) \sin\theta \\
&\quad + (2k_{nu} - 3k_{nv}) \cos\theta \sin^2\theta + k_{nu} \cos^3\theta \\
B_2 &= -2\tau_{gu} \sin^2\theta \cos\theta + \left(-k_{n\beta} + k_{nv} \cos^2\theta\right) \sin\theta + k_{nu} \sin^3\theta \\
B_3 &= k_{nv} \sin^3\theta + \left((7k_{nu} - 6k_{nv}) \cos^2\theta + k_{nv} - k_{n\beta} - k_{nu}\right) \sin\theta \\
&\quad - 2\tau_{gu} \cos\theta + 2\tau_{gu} \cos^3\theta \\
B_4 &= (-3k_{nu} + 2k_{nv}) \cos\theta \sin^2\theta - 2\tau_{g\alpha} \sin\theta \\
&\quad + (k_{n\alpha} + k_{nv} - k_{nu}) \cos\theta + (2k_{nu} - 3k_{nv}) \cos^3\theta - 2\tau_{gu} \sin^3\theta \\
B_5 &= \sin\theta \left((-k_{nu} + k_{nv}) \cos\theta \sin\theta - 2\tau_{gu} \cos^2\theta + \tau_{g\alpha} + \tau_{gu}\right) \\
B_6 &= \cos\theta \left(-2\tau_{gu} \cos^2\theta + (-k_{nu} + k_{nv}) \sin\theta \cos\theta + \tau_{g\alpha} + \tau_{gu}\right)
\end{aligned}$$

$$\begin{aligned}
C_1 &= -k_{g\alpha} + k_{gu} \cos\theta + k_{gv} \sin\theta \\
C_2 &= -k_{g\beta} - k_{gu} \sin\theta + k_{gv} \cos\theta
\end{aligned}$$

https://doi.org/10.1017/S026357471700008X Published online by Cambridge University Press

Appendix B

$$f_1\left(\sigma,\varphi,\omega'_3\right)=\omega'_3\left(-0.092+0.033\sin 2\varphi+0.1157\cos^2\varphi\right)$$
$$+\sigma\begin{pmatrix}-1.013-2.765\cos^2\varphi-1.074\cos^3\varphi+5.041\sin^3\varphi-0.894\cos 2\varphi+0.564\cos 4\varphi\\-13.93\sin 2\varphi+1.079\sin 4\varphi+0.051\cos 3\varphi+0.051\sin 3\varphi-4.228\cos\varphi+4.829\sin\varphi\end{pmatrix}$$
$$f_2\left(\sigma,\varphi,\omega'_3\right)=\omega'_3\left(-0.225-0.13\sin 2\varphi+0.171\cos^2\varphi\right)$$
$$+\sigma\begin{pmatrix}0.9116-1.726\cos^2\varphi-0.123\cos^3\varphi-2.418\sin^3\varphi+0.322\cos 2\varphi-0.192\cos 4\varphi\\+5.84\sin 2\varphi-0.476\sin 4\varphi-0.03\cos 3\varphi-0.03\sin 3\varphi+1.965\cos\varphi-0.88\sin\varphi\end{pmatrix}$$
$$f_3\left(\sigma,\varphi,\omega'_3\right)=\omega'_3\left(-0.178+0.079\sin 2\varphi+0.234\cos^2\varphi\right)$$
$$+\sigma\begin{pmatrix}6.831-13.11\cos^2\varphi-1.943\cos^3\varphi-2.002\sin^3\varphi+0.419\cos 2\varphi+0.217\cos 4\varphi\\+5.722\sin 2\varphi-0.702\sin 4\varphi+3.383\cos\varphi-1.839\sin\varphi\end{pmatrix}$$
$$f_4\left(\sigma,\varphi,\omega'_3\right)=\sigma\begin{pmatrix}0.207+0.385\cos^2\varphi-0.196\cos^3\varphi+0.112\cos 4\varphi+0.227\sin 4\varphi\\+0.624\cos\varphi+2.196\sin\varphi-5.783\cos\varphi\sin\varphi-0.992\cos^2\varphi\sin\varphi\end{pmatrix}$$
$$f_5\left(\sigma,\varphi,\omega'_3\right)=\sigma\begin{pmatrix}7.259-13.49\cos^2\varphi-2.356\cos^3\varphi+0.55\cos 4\varphi-0.225\sin 4\varphi\\+6.183\cos\varphi+1.798\sin\varphi-1.844\cos\varphi\sin\varphi-0.298\cos^2\varphi\sin\varphi\end{pmatrix}$$
$$f_6\left(\sigma,\varphi,\omega'_3\right)=\sigma\begin{pmatrix}-1.0+1.857\cos^2\varphi-0.238\cos^3\varphi+0.196\cos 4\varphi+0.501\sin 4\varphi\\-2.114\cos\varphi+4.546\sin\varphi-12.19\cos\varphi\sin\varphi-2.138\cos^2\varphi\sin\varphi\end{pmatrix}$$

References

1. H. Yousef, M. Boukallel and K. Althoefer, "Tactile sensing for dexterous in-hand manipulation in robotics—a review," *Sensors Actuators A: Phys.* **167**(2), 171–187 (2011).
2. A. Sudsang and T. Phoka, "Regrasp Planning for a 4-Fingered Hand Manipulating a Polygon," *Proceedings of the IEEE International Conference on Robotics and Automation, 2003, ICRA'03*, Taibei, Taiwan (Sep. 14–19, 2003) pp. 2671–2676.
3. N. C. Dafle, A. Rodriguez, R. Paolini, B. Tang, S. S. Srinivasa, M. Erdmann, M. T. Mason, I. Lundberg, H. Staab and T. Fuhlbrigge, "Extrinsic Dexterity: In-Hand Manipulation with External Forces," *2014 IEEE International Conference on Robotics and Automation (ICRA)*, Hong Kong, China (May 31–Jun. 7, 2014) pp. 1578–1585.
4. N. Furukawa, A. Namiki, S. Taku and M. Ishikawa, "Dynamic Regrasping using a High-Speed Multifingered Hand and a High-Speed Vision System," *Proceedings of the 2006 IEEE International Conference on Robotics and Automation, 2006, ICRA 2006*, Orlando, FL, USA (May 15–19, 2006) pp. 181–187.
5. M. Cherif and K. K. Gupta, "3D in-Hand Manipulation Planning," *Proceedings of the 1998 IEEE/RSJ International Conference on Intelligent Robots and Systems, 1998*, vol. 141, Victoria, British Columbia, Canada (Oct. 13–17, 1998) pp. 146–151.
6. M. Kondo, J. Ueda and T. Ogasawara, "Recognition of in-hand manipulation using contact state transition for multifingered robot hand control," *Robot. Auton. Syst.* **56**(1), 66–81 (2008).
7. D. Rus, "In-hand dexterous manipulation of piecewise-smooth 3-D objects," *Int. J. Robot. Res.* **18**(4), 355–381 (1999).
8. A. Sudsang and N. Srinivasa, "Grasping and in-hand manipulation: Geometry and algorithms," *Algorithmica* **26**(3–4), 466–493 (2000).
9. J. Ueda, M. Kondo and T. Ogasawara, "The multifingered NAIST hand system for robot in-hand manipulation," *Mech. Mach. Theory* **45**(2), 224–238 (2010).
10. C. Exner, "Development of hand functions," **In**: *Occupational therapy for children* (P. N. Pratt and A. S. Allen, eds.), (Mosby, St. Louis, 1989) pp. 235–259.
11. C. Pehoski, A. Henderson and L. Tickle-Degnen, "In-hand manipulation in young children: Rotation of an object in the fingers," *Am. J. Occup. Therapy* **51**(7), 544–552 (1997).
12. H. Jeong and J. Cheong, "In-Hand Rolling Motion Planning using Independent Contact Region (ICR) with Guaranteed Grasp Quality Margin," *2013 IEEE International Conference on Robotics and Automation (ICRA)*, Karlsruhe, Germany (May 6–10, 2013) pp. 3239–3244.
13. Y. B. Kim, G. Kang, G. K. Yee, A. Kim, W. S. You, Y. H. Lee, F. Liu, H. Moon, J. C. Koo and H. R. Choi, "Exploration and reconstruction of unknown object by active touch of robot hand," *Intell. Service Robot.* **8**(3), 141–149 (2015).

https://doi.org/10.1017/S026357471700008X Published online by Cambridge University Press

14. M. F. Reis, A. C. Leite, F. Lizarralde and L. Hsu, "Kinematic Modeling and Control Design of a Multifingered Robot Hand," *2015 IEEE 24th International Symposium on Industrial Electronics (ISIE)*, Buzios, Rio de Janeiro, Brazil (Jun. 3–5, 2015) pp. 638–643.
15. H. van Hoof, T. Hermans, G. Neumann and J. Peters, "Learning Robot in-Hand Manipulation with Tactile Features," *2015 IEEE-RAS 15th International Conference on Humanoid Robots (Humanoids)*, Seoul, Korea (South) (Nov. 3–5, 2015) pp. 121–127.
16. Z. Doulgeri and L. Droukas, "On Rolling Contact Motion by Robotic Fingers Via Prescribed Performance Control," *2013 IEEE International Conference on Robotics and Automation (ICRA)*, Karlsruhe, Germany (May 6–10, 2013) pp. 3976–3981.
17. L. Droukas and Z. Doulgeri, "Rolling contact motion generation and control of robotic fingers," *J. Intell. Robot. Syst.* **1**, 1–18 (2015).
18. L. Cui and J. S. Dai, "A Coordinate-Free Approach to Instantaneous Kinematics of Two Rigid Objects with Rolling Contact and Its Implications for Trajectory Planning," *IEEE International Conference on Robotics and Automation*, Kobe, Japan (May 12–17, 2009) pp. 612–617.
19. L. Cui and J. S. Dai, "A darboux-frame-based formulation of spin-rolling motion of rigid objects with point contact," *IEEE Trans. Robot.* **26**(2), 383–388 (2010).
20. L. Cui and J. S. Dai, **In**: *Geometric Kinematics of Point Contact* (J. Lenarčič and M. M. Stanisic, eds.) (Springer, New York, US, 2010) pp. 429–436.
21. L. Cui and J. S. Dai, "A polynomial formulation of inverse kinematics of rolling contact," *J. Mech. Robot.* **7**(4), 041003_041001–041009 (2015).
22. L. Cui and J. S. Dai, "From sliding–rolling loci to instantaneous kinematics: An adjoint approach," *Mech. Mach. Theory* **85**(0), 161–171 (2015).
23. C. Cai and B. Roth, "On the planar motion of rigid bodies with point contact," *Mech. Mach. Theory* **21**(6), 453–466 (1986).
24. D. J. Montana, "The kinematics of contact and grasp," *Int. J. Robot. Res.* **7**(3), 17–32 (1988).
25. A. Marigo and A. Bicchi, "Rolling bodies with regular surface: Controllability theory and application," *IEEE Trans. Autom. Control* **45**(9), 1586–1599 (2000).
26. L. Cui, "Differential Geometry Based Kinematics of Sliding-Rolling Contact and Its Use for Multifingered Hands," **In**: *Centre for Robotics Research* (King's College London, London, UK, 2010).
27. C. S. Hwang, M. Takano and K. Sasaki, "Kinematics of grasping and manipulation of a B-spline surface object by a multifingered robot hand," *J. Robot. Syst.* **16**(8), 445–460 (1999).
28. J. C. Trinkle and R. P. Paul, "Planning for dexterous manipulation with sliding contacts," *Int. J. Robot. Res.* **9**(3), 24–48 (1990).
29. I. Kao and M. R. Cutkosky, "Quasistatic manipulation with compliance and sliding," *Int. J. Robot. Res.* **11**(1), 20–40 (1992).
30. M. Vatani, E. D. Engeberg and J.-W. Choi, "Detection of the position, direction and speed of sliding contact with a multi-layer compliant tactile sensor fabricated using direct-print technology," *Smart Mater. Struct.* **23**(9), 095008 (2014).
31. M. Vatani, E. D. Engeberg and J.-W. Choi, "Force and slip detection with direct-write compliant tactile sensors using multi-walled carbon nanotube/polymer composites," *Sensors Actuators A: Phys.* **195**, 90–97 (2013).
32. A. M. Okamura, N. Smaby and M. R. Cutkosky, "An Overview of Dexterous Manipulation," *Proceedings of the IEEE International Conference on Robotics and Automation, 2000, ICRA '00*, vol. 251, San Francisco, CA, USA (Apr. 24–28, 2000) pp. 255–262.
33. R. M. Murray, Z. Li and S. S. Sastry, *A Mathematical Introduction to Robotic Manipulation* (CRC Press, Boca Raton, USA, 1994).
34. F. C. Park and R. W. Brockett, "Kinematic dexterity of robotic mechanisms," *Int. J. Robot. Res.* **13**(1), 1–15 (1994).
35. R. W. Brockett, *Robotic Manipulators and the Product of Exponentials Formula* (Springer, Berlin, 1984).
36. L. Romdhane and J. Duffy, "Kinestatic analysis of multifingered hands," *Int. J. Robot. Res.* **9**(6), 3–18 (1990).
37. L. Cui and J. S. Dai, "Posture, workspace, and manipulability of the metamorphic multifingered hand with an articulated palm ASME," *J. Mech. Robot.* **3**(2), 021001_021001–021007 (2011).
38. L. Cui and J. S. Dai, "Reciprocity-based singular value decomposition for inverse kinematic analysis of the metamorphic multifingered hand ASME," *J. Mech. Robot.* **4**(3), 034502_034501_034506 (2012).
39. L. Cui, U. Cupcic and J. S. Dai, "An optimization approach to teleoperation of the thumb of a humanoid robot hand: Kinematic mapping and calibration," *J. Mech. Des.* **136**(9), 091005_091001_091007 (2014).
40. L. Cui, T. Tan, K. D. Do and P. Teunissen, "Challenges and solutions for autonomous robotic mobile manipulation for outdoor sample collection," *J. Electr. Electron. Eng.* **3**(5), 156–164 (2015).
41. E. Cartan, *Riemannian Geometry in an Orthogonal Frame* (World Scientific Press, Singapore, 2002).
42. H. Cartan, *Differential Forms* (Dover Publisher, New York, 1996).
43. M. P. Carmo, *Differential Geometry of Curves and Surfaces* (Prentice-Hall, Englewood Cliffs, 1976).
44. A. Gray, *Modern Differential Geometry of Curves and Surfaces with Mathematica* (CRC Press, Inc., Boca Raton, Florida, 1996).
45. G. Wei, J. Sun, X. Zhang, D. Pensky, J. Piater and J. S. Dai, "Metamorphic Hand based Grasp Constraint and Affordance," *ASME 2015 International Design Engineering Technical Conferences and*

Computers and Information in Engineering Conference, American Society of Mechanical Engineers, Boston, Massachusetts, US (Aug. 2–5, 2015) pp. V05BT08A008–V005BT008A008.
46. J. S. Dai and D. R. Kerr, "Analysis of force distribution in grasps using augmentation," *J. Mech. Eng. Sci.* **210**(1), 15–22 (1996).
47. J. S. Dai and J. Rees Jones, "Interrelationship between screw systems and corresponding reciprocal systems and applications," *Mech. Mach. Theory* **36**(5), 633–651 (2001).
48. J. S. Dai, D. Wang and L. Cui, "Orientation and workspace analysis of the multifingered metamorphic hand-metahand," *IEEE Trans. Robot.* **25**(4), 942–947 (2009).
49. M. T. Mason, *Mechanics of Robotic Manipulation* (MIT Press, Cambridge, Massachusetts, 2001).
50. J. C. Trinkle, "A Quasi-Static Analysis of Dextrous Manipulation with Sliding and Rolling Contacts," *Proceedings of the 1989 IEEE International Conference on Robotics and Automation, 1989*, (1989) pp. 788–793.
51. M. Cherif and K. K. Gupta, "Planning quasi-static fingertip manipulations for reconfiguring objects," *IEEE Trans. Robot. Autom.* **15**(5), 837–848 (1999).

https://doi.org/10.1017/S026357471700008X Published online by Cambridge University Press